BACHELOR' S THESIS / BIOMEDICAL ENGINEERING 2022

Study of the propensity to suffer an osteoporotic hip fracture based on biomechanical parameters and the automatic selection of the region of interest

Berta Mateu Yus

upf. Universitat Pompeu Fabra Barcelona

Study of the propensity to suffer an osteoporotic hip fracture based on biomechanical parameters and the automatic selection of the region of interest

Berta Mateu Yus

Bachelor's thesis UPF 2021/2022

Thesis supervisor(s):

Pr. Carlos Ruiz Wills, (Department of Information and Communication Technologies (DTIC), UPF)

Pr. Simone Tassani, (Department of Information and Communication Technologies (DTIC), UPF)

Acknowledgments

During these last nine months, I have had the honor to have as supervisors of my thesis Dr. Carlos Ruiz Wills and Dr. Simone Tassani. I would like to acknowledge their unconditional support, guidance, and knowledge received from them. Thanks to them, I have been able to learn and develop new skills that complemented the ones acquired during this degree. It has been a privilege to work along with such talented and dedicated researchers.

I would also like to acknowledge Dr. Andy Olivares and Marina Estévez from University Pompeu Fabra for agreeing to be the external reviewers of my thesis.

Lastly, I want to express my gratitude to all the members of the BCN Medtech group. For their advice, for challenging me and encouraging me to improve and always go one step further.

Abstract

Osteoporotic hip fractures represent a high social and economic burden. As such, the identification of the fracture risk for a patient is of high interest to clinicians. Femur finite elements 3D models based on advanced DXA imaging allowed us to discriminate between fracture and non-fracture cases. However, the effectiveness of such methods is very sensible to the selection of the analysis region. This project aims to evaluate the power of classification of biomechanical parameters obtained through those models, focused on automatized ROI selection using advanced statistical methods. A cohort of 180 patients, 90 control and 90 fracture, were used, considering an equal balance between men and women. Proximal femur 3D models were obtained from advanced DXA acquisitions, having the same correspondence of nodes and elements. Lateral fall was simulated by the application of a patient-specific force at the top of the femoral head, the trochanter was fixed in the direction of the force and the distal area was fully constrained. Five parameters were evaluated: volumetric bone mineral density (vBMD), maximum principal stress/strain and major principal stress/strain. The critical areas were selected by using a statistical parametric map based on random field theory to evaluate the power of classification of the parameters. The results showed 100% accuracy when predicting trochanteric fractures and a 93.3% for neck fractures. By gender separation, 100% prediction accuracy for the neck fractures. When considering only vBMD, a 100% and 81.7% accuracy on the predictions for trochanter and neck fractures respectively was reached. Although the prediction using the outcomes of the FEM give perfect prediction, this tool is far from the clinics. However, by only considering vBMD, which can be obtained from de DXA based model without the need of lateral fall simulation, good prediction can be obtained. This opens us the possibility to provide a preventive treatment to those patients with a prediction of risk of fracture. This way the social and economic burden of this medical condition would be reduced.

Keywords

Osteoporosis, femur, hip fracture, neck, trochanter, bone mineral density, critical region, random field theory, finite element model.

Prologue

Osteoporotic hip fractures is a medical condition that is more and more frequent among elder people since1 in 3 women and 1 in 5 men will sustain an osteoporotic hip fracture in their lifetime. This type of fracture usually has consequences of disability, chronic pain, reduced quality of life, and higher mortality risk.

To be able to predict the risk of suffering from an osteoporotic hip fracture, would allow the clinician to treat the patients to prevent these fractures. Through finite element models, different predictive models have been developed, however, the selection of the region under study has been the key point. This selection is usually subjective.

This project presents an innovative way to automatically select those regions that may be more informative when predicting those fractures. With this methodology, an improvement on the accuracy of the prediction form previous studies have been achieved which has proven the importance of the selection of the region under study

This study could be a game-changer in the prevention of the osteoporotic hip fracture as it can potentially lead to a clinical tool used to evaluate the risk of suffering an osteoporotic hip fracture. Being able to predict this risk could allow the clinicians to take preventive measures and this way, reduce the number of this type of fractures.

Index

List of figures

List of tables

1.Introduction

1.1 The problem and motivation:

With the advances in medicine nowadays people can live longer. However, with longer longevity, the percentage of old age-associated diseases increases within the population.

A medical condition that is more and more frequent among elder people is osteoporotic hip fracture. It has been estimated that 1 in 3 women and 1 in 12 men will sustain a hip fracture in their lifetime [1]. However, 86% of these hip fractures occur in individuals aged 65 years older [2]. Within all these fractures, it has been estimated that 51% of fractures in women and 24% of fractures in men are attributed to osteoporosis [3]. The usual consequences of suffering this type of fracture are disability, chronic pain, reduced quality of life, and higher mortality risk. It has been estimated that 20-30% of people who suffer a hip fracture die in the first year after the fracture [4]. From the health expenses point of view, it was estimated that within the first year in Spain, the treatment of osteoporotic fractures has a cost of around 9000€ and it increases in the following years [5]. Considering that the number of osteoporotic hip fractures increases with the current trend of population aging, the total money invested in the treatment of this category of fracture for all the population is huge.

It is essential to find a way to prevent these osteoporotic hip fractures to reduce the social and economic burden of people suffering from them. Although with the pharmacological advances there are osteoporosis treatments that may reduce the risk of fracture up to 50% [6], there is the need of identifying those patients who are at risk. This way, those patients who are really at risk can be treated in advance. Nevertheless, the first step to prevent these fractures is to first diagnosis the osteoporosis disease.

Diagnostic tools for osteoporosis are mainly based on the measurement of bone mineral density (BMD). Three main image techniques allow the BMD measurement. The gold standard is the Dual X-Ray absorptiometry (DXA), which offers a 2D representation of the BMD of the region. Yet quantitative computed tomography (CT) [7] and quantitative ultrasound (QUS) also offer the possibility of measuring the BMD [8].

Nowadays, there are tools in the market that allow this prediction. FRAX is a computer-based algorithm that calculates the 10-year probability of a major osteoporotic fracture with a 70% of accuracy. Apart from the fact that its accuracy implies a 30% of error which is a high percentage, it also presents other limitations that will later be explained [9].

Thanks to medical imaging, patient-specific models of osteoporotic proximal femur can be generated. Finite element (FE) models allow to simulate different mechanical condition [10], including side-way lateral fall. Such models seek a criterion to predict the fracture. Several studies had used the models, nevertheless, the results obtained are not as homogeneous to stablish a general criterion. Generally, in these models statistical

techniques and machine learning (ML) algorithms have been used to obtain the classification criterion for fracture. One aspect that is variable within the different studies is the selection of the region of analysis. The selection of the region under study is very subjective and has significant effects on the accuracy of the classification outcomes. In a study published by Ruiz Wills et. al [11], they suggested the hypothesis that some specific regions can be automatically selected that are more informative in terms of prediction of the fracture. These so-called critical regions might not be the fracture regions

A recent study [12] developed a methodology that proved that by employing statistical Random Field Theory (RFT) the critical region in femur finite elements models can be found. This methodology was then applied to a dataset of osteoporotic subjects and high classification accuracies were obtained. A limitation of this study was that analysis was applied in an unbalanced dataset. The number of fracture and control cases was not the same, and the lack of male patients made them be removed from the study. Performing a statistical analysis with an unbalanced dataset often implies poor extrapolation of the outcomes obtained. The combination of balance data with the RFT methodology in 3D modeling might provide a better understanding of hip fracture and the development of tools for its prediction.

1.2 Objective

Hence, the aim of this study is to evaluate the power of classification of biomechanical parameters obtained through DXA-based 3D femur finite elements models focusing on the analysis of the critical region obtained through RFT to better identify those osteoporotic patients with propensity to suffer a hip fracture.

2. State of the art

2.1 Bone tissue:

Bone tissue is a mineralized and viscous-elastic tissue in charge of supporting and protecting the body and storing minerals. The matrix of bone is composed of organic materials such as collagen, proteins, proteoglycans, and water, and inorganic materials being the hydroxyapatite the most relevant one [13]. It can remodel its structure. This remodeling process is controlled by cells and can be altered by either mechanical [14] or organic stimulus.

2.1.1 Cortical bone

Cortical bone (Figure 1d) is a dense tissue located in the outer part of bones. It represents 80% of the total bone mass [15]. It oversees supporting the body and protecting the organs as well as storing calcium. Its structure is composed by microcolumns called osteons which give this tissue the anisotropic behavior. The arranged collagen fibers grant the cortical bone a higher resistance to longitudinal forces, and within the longitudinal forces, the mineral matrix allows greater resistance to compression loads [16].

2.1.2 Trabecular bone

The trabecular bone (Figure 1b) is a highly porous anisotropic material that is found in the inner layer of all bones. This tissue is where the hematopoiesis takes place, thus it is a high vascularized tissue. It is made of trabeculae which give the porous structure. The trabeculae oriented themselves in a way that they can better support the load applied in that region. Therefore, unlike cortical bone, in the trabecular bone, the anisotropy is heterogeneous, and depending on the region, the direction that can support graters load will change [16]. Trabecular bone has a higher strain index than cortical bone, which provides it with more elasticity, nevertheless, it can support less load for a unit of area [5]. In the image below, the differences in structure of the cortical and trabecular bone can be seen.

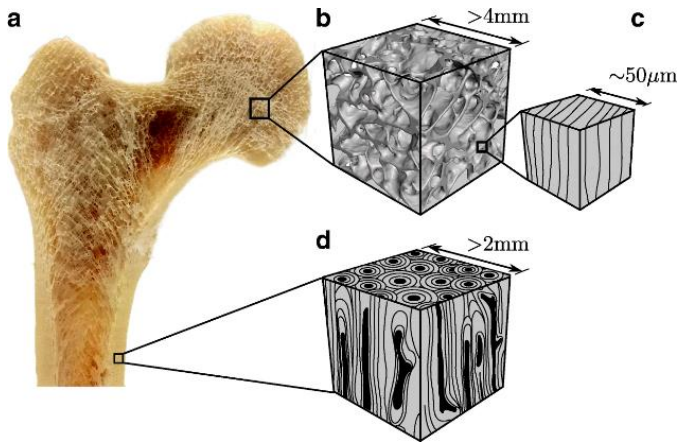

Figure 1: a) Cross section of the human proximal femur showing the trabecular region and cortical shell. b) Representative volume element (RVE) of the trabecular network and c) RVE of bone tissue of single trabeculae. d) Representative volume element of cortical

2.2 Proximal Femur

The femur is classified as a long bone; therefore, it has one diaphysis and two epiphyses. The body of the bone (diaphysis) is formed by compact bone walls and in its interior, there is the medullary cavity, containing the bone marrow. The extremes of the bone (epiphysis) are formed by trabecular bone covered with a thin layer of cortical bone [17]. The bone surface, except the joint's regions, is covered with a fibrous membrane called the periosteum. The periosteum contains blood vessels, nerves, and lymphatic vessels that nourish compact bone. The region of the epiphysis that forms joints is covered with articular cartilage, a thin layer of cartilage that reduces friction and acts as a shock absorber.

As shown in Figure 2, the proximal femur includes the femoral head, neck, and region 5-cm distal to the lesser trochanter. There is a 125°–130° inclination angle between the head and neck and the femoral body [17].

- **Head:** articulates with the acetabulum of the pelvis to form the hip joint. It has a smooth surface covered with articular cartilage [18].
- **Neck:** connects the head of the femur with the shaft.
- **Intertrochanteric area:** distal to the femoral neck and proximal to the femoral shaft. It is the area where the femur changes from an essentially vertical bone to a bone angling at a 45° angle from the near-vertical to the acetabulum or pelvis [19].
- **Greater trochanter:** lateral palpable projection of bone that originates from the anterior aspect, just lateral to the neck. It's the attachment site for five muscles of the gluteal region.
- **Lesser trochanter:** projects from the posteromedial side of the femur, just inferior to the neck-shaft junction. It is the site of attachment for iliopsoas muscle.

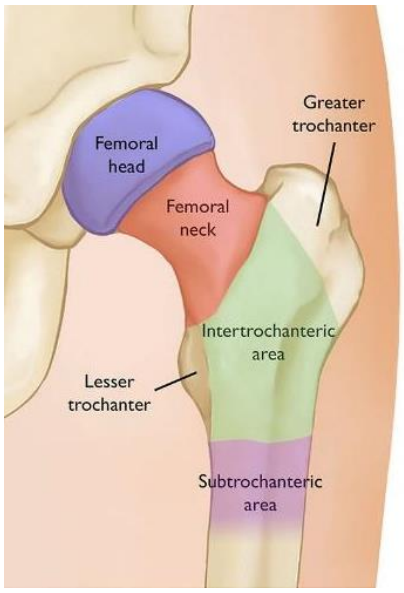

Figure 2: Proximal femur parts [11]

2.3 Osteoporosis

Osteoporosis is defined as a systemic skeletal disease characterized by low bone mass and microarchitectural deterioration of bone tissue with a consequent increase of bone fragility and susceptibility to fractures [20] (see Figure 3), the most common ones are wrists, vertebral and hip fractures [4]. This deterioration of the bone is due to the loss of homeostasis in the bone remodeling process meaning that an imbalance of bone resorption and bone formation is what causes osteoporosis. In a healthy patient, the bone is constantly remodeling and replacing old bone with new bone thanks to the action of osteoclasts, osteoblast. On the one side, osteoblasts, which are derived from multipotent mesenchymal stem cells, are in charge of synthesizing new bone, and on the other side, osteoclasts, which are formed from hematopoietic stem cells, are the ones in charge of bone reabsorption. The development of these two types of cells is controlled by a network of growth factors and cytokines produced in the bone level, systemic hormones, and also molecules that mediate cell-cell and cell-matrix interactions [21].

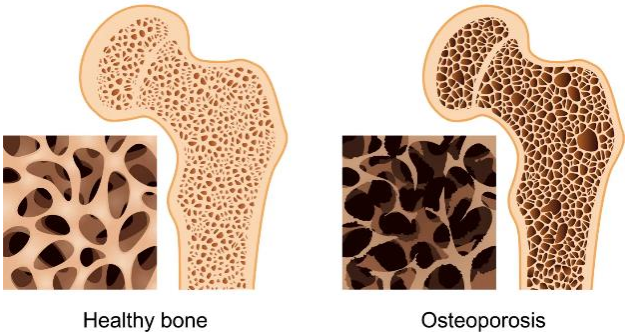

Figure 3: Difference between healthy bone and osteoporotic bone.
From https://medpacblog.wordpress.com/2016/10/07/osteoporosis/

2.3.1 Main causes of osteoporosis

The causes of osteoporosis can be classified into two different types:

- **Primary causes:** when is a consequence of the aging process [22]. The phenomenon of aging itself reduces the amount of bone formed during bone remodeling and that is why the highest percentage of people who suffer from an osteoporotic hip fracture are over 65 years old [2]. A second age-related phenome that causes osteoporosis, is the loss of production of sex hormones which have a protective effect on bone since they regulate the development of cells in the bone marrow [21]. Women are the ones more affected since during menopause hormones such as estrogen and progesterone decline.

- **Secondary causes:** when an underlying medical condition or the use of a certain medication interferes with the body's ability to produce new bone tissue [22]. The most common secondary cause of osteoporosis is glucocorticoid-induced. Glucocorticoids (GC) are hormones that are used to treat inflammatory or autoimmune disorders. Glucocorticoids are systematically produced in our body, however, at high concentrations, they decrease bone production causing bone loss. [23]. This phenomenon is the main origin of osteoporosis among people above 50-year-old [21].

2.3.2 Diagnosis

The goal standard to diagnose osteoporotic hip fractures and hip fracture assessment is through bone mineral density (BMD). As mentioned earlier, bone is partially composed of a mineral, BMD is the amount of bone mineral in bone tissue. There are BMD tests that measure bone density and compare them to a standard score. The most common score is the T-score, which is when the measure is compared with the measure of a healthy adult, and the difference in value is expressed in standard deviation (SD) units. A T-score lower than 1 SD is considered normal, and a value above 2.5 SD means osteoporosis [24].

Three main imaging techniques allow the BMD measurement.

- **Quantitative ultrasound (QUS)**: This is a non-ionizing, fast, relatively inexpensive, and imaging technique but it is not used routinely for the diagnosis of osteoporosis [25].

- **Quantitative computed tomography (QCT)**: Although this technique allows obtaining a volumetric distribution of the BMD and differentiation between cortical and trabecular bone, it implies higher doses of radiation [26, 27] and it is considerably more expensive [27] so it is not that frequently used in the medical environment.

- **Dual-Energy X-Ray Absorptiometry (DXA)** [24, 26, 27]: It is the gold standard. I consist of low-dose x-rays with two distinct energy peaks sent through the body. By using two sources of energy, the bone measurement is more accurate [28, 29]. This technique allows a 2D measurement of the bone density distribution. Although it is cheap and has low radiation, it does not allow obtaining a volumetric distribution of the BMD [26, 27].

2.4 Osteoporotic hip fracture

Osteoporotic hip fractures can be classified into two groups depending on the anatomical region where the fracture occurred (see Figure 4).

- **Intracapsular fractures**: occur within the fracture of the hip joint. Fractures of the femoral head and neck are intracapsular. These fractures could be likely to damage the blood supply leading to fatal consequences such as avascular necrosis [30].

- **Extracapsular fractures:** occurs outside the articulation capsule. Intertrochanteric and subtrochanteric fractures are extracapsular. It's been stated that trochanteric fractures are more associated with osteoporosis [4].

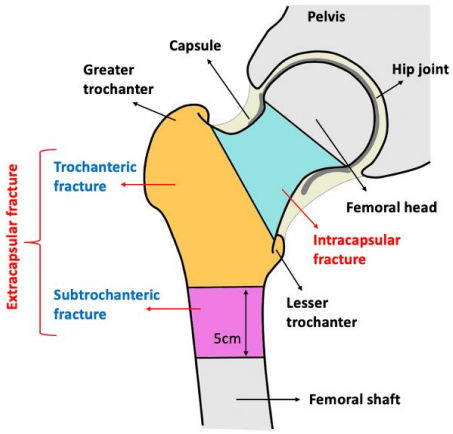

Figure 4: Image showing the different regions where each type of fracture occurs [29].

2.5. Strategies to tackle the Hip fracture

Even though BMD measured by DXA measurement is the goal standard, when diagnosing osteoporosis, it only has a 65% of accuracy when predicting osteoporotic hip fracture which is not enough [31]. Currently, no tool allows physicians to perform exact predictions on whether a patient will suffer or not an osteoporotic hip fracture, however, several techniques have been developed during the past years to obtain more precise results.

2.5.1 Fracture risk assessment tool (FRAX)

For the prediction of hip fracture, there are already available tools. FRAX is a computer-based algorithm that calculates the 10-year probability of a major osteoporotic fracture; however, it has been argued the reliability of the predictions since many relevant variables are not considered in this algorithm like the difference between races or ethnicities [9]. Also, another limitation is that most of the input parameters are absolute, and not dose/frequency-dependent.

2.5.2 Finite element models

With medical images, it is possible to generate patient-specific Finite element models (FEM) and study the behavior of the bone and the fracture in a virtual way. FEM consists of the discretization of a large system in a finite number of elements by creating a mesh and solving the mathematical equations in the nodes and interpolating to all the other points of the model. With FEM, approximate results are obtained [10, 32].

To validate that FEM was accurate when simulating a fracture in an osteoporotic hip, Felps et. al [33] compared an experimental model of a hip fracture using a cadaveric bone and surrogate soft tissue to a FEM of two patients. After the study was completed, they stated that the FEM closely matched the experimental model. Using only FEM, no prediction of hip fracture is possible since the dimensionality of the output can be high (lots of elements and variables). That is why several studies have focused on post-processing the data obtained in the simulations to be able to establish a criterion to predict osteoporotic hip fractures.

Aldieri et. al [34] studied which parameters were related to hip fractures. According to the strain-based bone fracture criteria, the minimal and maximal principal strains were extracted at each element centroid to calculate the Risk Factor (RF). The regions with a higher RF were the femur's neck and intertrochanteric. Following, they performed an Akaike information criterion (AIC) based multivariate linear regression analysis that led to the identification of the optimal combinations of hip structural analysis (HSA) variables, suitable to predict the extracted higher superficial RF. The parameters related to the fracture that they obtained were the following: in the narrow neck region the neck shaft and the bulking ratio and in the femoral shaft region the neck-shaft angle and the cross-sectional area.

Villamor et. al [31] performed a machine learning (ML) analysis. They considered 39 patient-specific variables that were related to clinical data, geometrical attributes, fall-related attributes, bone density, and FE analysis outputs. From all these attributes, they only kept the ones with a Pearson correlation lower than 0.8, leaving them with 19 attributes, and those attributes were used as an input for a support vector machine (SVM) algorithm. From this study, they conclude that the prediction of the fractures could be considerably improved when clinical 2D patient-specific mechanical data is introduced into a ML classifier.

Recently, Ruiz Wills et. al [27], used statistical analysis to determine which of the output parameters of the FEM could be used as a good classifier. First, they did an ANOVA,

which evaluated the influence of the factors extracted from the FE simulation. Only in the case where the null hypothesis was rejected, the factors were considered as input values for the receiver operative characteristic (ROC) curve method. With this method, they were able to determine which factors were good classifiers for predicting the osteoporotic hip fracture. They obtained that the major principal stresses (MPS) were the best classifier. Nevertheless, that study had some limitations, in this case, the data was not balanced since there were 30 male and 81 female subjects. In a later study done by the same research team [11], they followed the same methodology, however, they only analyzed the regions with higher MPS. Only analyzing this concrete region, the AUC values of the ROC increased.

With this study, it was proven that the selection of the region affects the accuracy of the classification. They established that there are regions that are more informative when predicting the fracture, the critical regions (CR). By analyzing the CR, the noisy elements would be omitted during the analysis and better results could be obtained.

In a master's thesis [12], the methodology to automatically find the critical regions using statistical Random Field Theory Analysis was established. Nevertheless, the analysis of this CR was done using an unbalance dataset the same one as in [27]. They obtained accuracies of 79% when predicting neck fracture and 89% in trochanter fracture. Because the data analyzed was from an unbalance dataset, the classification accuracies obtained could not be generalized. That is why a study using a balanced dataset is needed to obtain a generalizable prediction of the risk of the fracture using the biomechanical parameters of the CR.

2.6. Statistical parametric map

Statistical Parametric Maps (SPM) are images or fields with values that are, under the null hypothesis, distributed according to a known probability density function, usually the Student's t or F-distributions [35].

Often, when performing and statistical analysis, it is not known in advanced where to look for an effect and therefore, the whole set of data end up being analyzed instead of focusing only on specific regions. Random Field Theory (RFT) is a tool used in statistical analysis of SPM that allows the detection of an effect at an unknown spatial location and presents a solution to the multiple comparisons problem [36].

2.6.1 Multiple comparison problem

In statistics, to determine if there is a statistical relationship or significance between two variables the test of the null hypothesis (H_0) is used. If this hypothesis is accepted, this will mean that there is no effect between the variables, however, if the test is rejected an alternative hypothesis is accepted (H_1), which states that a statistical relationship between the independent variables exists. When rejecting the null hypothesis, an error must be considered since there is a chance that the statistic had arisen by chance. This error is usually around 5% and is called Type I error or alpha value (α) [37].

A problem arises when we perform a multiple comparison. If the null hypothesis test is performed for each independent variable (n), the overall probability of having a Type I error increases significantly in the overall dataset although the alpha value is set to 0.05 since the probability of having a Type I error for each value is accumulated. This will imply a higher error rate and a global error rate given that the probability of having a Type I error is set for the whole set of values, which mean that either the whole set rejects the null hypothesis or accepts it.

$$Prob\ Type\ I\ error = 1 - (1 - \alpha)^n \quad (1)$$

The family-wise error rate (FWE) is the likelihood that a family of values could have arisen by chance. A way to test this FWE, is by looking for any statistic values that are higher than what would be expected. For this, a threshold needs to be found and any value that go over this threshold are unlikely to have arisen by chance in terms of a probability value.

$$P^{FWE} = 1 - (1 - \alpha)^n \quad (2)$$

If we consider that α is small, we could rewrite the equation as:

$$P^{FWE} = n\alpha \quad (3)$$

2.6.2 Bonferroni correction

One of the most common strategies to control the Type I error rate, is the Bonferroni correction. This correction adjusts the α value for an individual test by dividing the P^{FWE} by the number of statistical test conducted (n):

$$\alpha = \frac{P^{FWE}}{n} \quad (4)$$

This correction assumes independent tests on the multiple comparison, so it is suitable for discrete data. When applied to test that have a correlation between neighboring statistic values, it become too conservative, meaning that although the Type I error rate is set, it may fail to reject the null hypothesis when should in fact reject it. This phenomenon is called Type II error or β [38].

2.6.3 Random field theory

Random field theory is a body of mathematics that has been versatile in dealing with the thresholding problems regarding the multiple comparison problems. This tool implements a methodology for correcting the p-value which considers the correlation between neighboring statistic values. This way, with the use of RFT, lower thresholds can be found in continuous data, finding the required FWE making it less conservative than in the Bonferroni correction.

The application of the RFT has 3 stages [37]:

1. **Estimate the smoothest (spatial correlation):** The goal of smoothing is to reduce the number of independent observations. The smoothness can be expressed as the width of the smoothing Gaussian kernel, known as 'full width of half maximum' (FWHM) (see Figure 5). From the FWHM the number of resells can be calculated. The term resels refers to a block of values that is the same size as the FWHM and it can be calculated using the following formula where V is the volume of the research region and D are the number of dimensions.

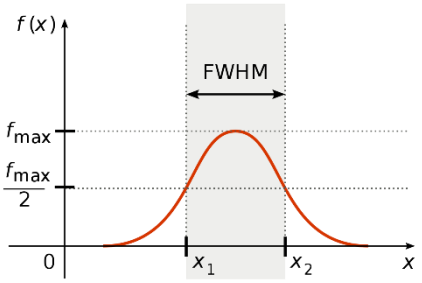

Figure 5: Full width of half maximum (FWHM)

$$Resel_D = \frac{V}{FWHM^D} \qquad (5)$$

2. **Calculate the expected Euler Characteristic from the smoothen data:** The expected Euler Characteristic ($E[EC]$) is approximately equivalent to the probability of a family wise error and it follows the formula:

$$P^{FWE} \approx E[EC] = R(4\log_e 2)(2\pi)^{-\frac{3}{2}} Z_t e^{-\frac{1}{2}Z_t^2} \qquad (6)$$

where R is the number of resels and Z_t is the Z score threshold. This threshold will have different values depending on the P^{FWE} desired and the smoothness applied in the data.

3. **Find the proper threshold:** Define the proper thresholds that reject erroneously the null hypothesis with the α value set by the user. When running a statistical test, the list of values higher than the threshold will be obtained, these values will be the ones statistically significant under the defined conditions.

3. Materials and methods

3.1 Subjects database

The dataset of the previous study [12] contained 111 osteoporotic patients over the age of 50, all from CETIR Medical Group, Hospital Mutua de Terrassa. In this dataset, there were considerably more female than male patients and more control than fractured cases see table 1. Within the fractured cases, two types of fractures were considered depending on where the fracture occurred, the trochanteric region and the neck region. From this

dataset, FE patient-specific static simulations had already been done and the following mechanical parameters for each element had been extracted:

- Volumetric density from DXA
- Major Principal Stress (MPS) [MPa]
- Major Principal Strain (MPE) [mm/mm]
- Maximum principal stress absolute [MPa]
- Maximum principal strain absolute [mm/mm]

To balance this data, 69 new patients with the same condition as the previous dataset were added to the dataset. From these new patients, patient-specific models and simulations of a lateral fall had to be done. To do this, the same methodology as in the models of the previous patient was used.

	Fracture				Control	
	Neck		Trochanter			
	Female	Male	Female	Male	Female	Male
Dataset from [12]	26	10	19	7	37	12
New database	0	16	0	12	8	33

	Male	Female
Total fracture	45	45
Total control	45	45

Table 1: Fracture and control cases from previous and new datasets

3.2 Generation of the model

3.2.1 Patient-specific model

The image acquisition of each patient was done as in [27], using GE Healthcare DXA bone densitometer to obtain the 2D image of de BMD. The 3D geometry was obtained from these DXA images using the 3D-shaper software[1].

From the 3D geometry, volumetric meshes follow the same steps as in [27]. The final meshes contained 126800 hexahedral elements and had always the same number of nodes and one-to-one correspondence. Since all the meshes had the same numeration of elements, that allowed the identification through the element numbers of the fracture regions, i.e., neck and trochanteric regions (see Figure 6a).

[1] https://www.3d-shaper.com/en/index.html

To later apply the different mechanical properties of the cortical and trabecular bone, two sections within the mesh were generated (see Figure 6b). A fine layer of three elements was created from the surface of the femur to the interior for the cortical bone, and the rest of the elements were considered trabecular bone.

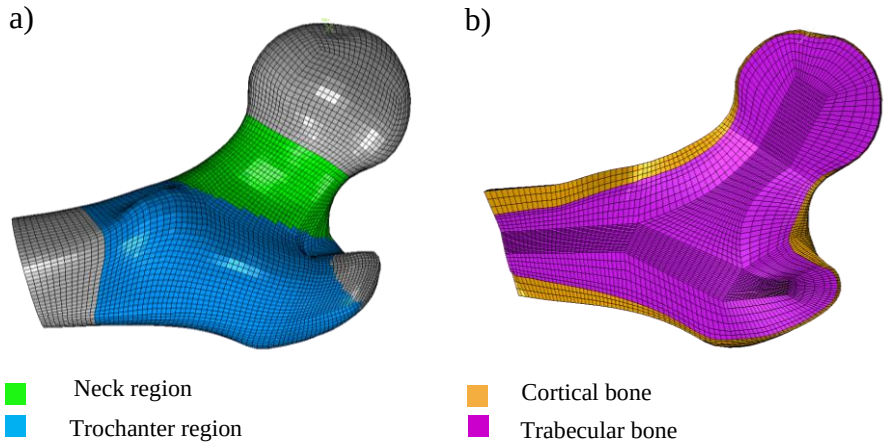

Figure 6: : a) Proximal femur with the trochanteric and neck regions highlighted, b) Volumetric mesh of a proximal femur with the differentiated sections of cortical and trabecular bone

3.2.2Mechanical properties

The bone tissue was considered linear isotropic elastic with a Poison's ratio of 0.3 [27]. The vBMD distribution was used to calculate the stiffness of each element of the bone. This is because within the equations used to calculate the different young's modulus. For the cortical and trabecular bone Young's modulus, two different equations were used [27]. The young modulus had as units MPa.

$$E_{cortical=}10200{\rho_{ash}}^{2.01} \quad (7)$$
$$E_{trabecular=}0.003715{\rho_{app}}^{1.96} \quad (8)$$

ρ_{ash} is the ash density of the bone measure in g/cm^3. The ρ_{ash} is calculates using ρ_{QCT} that is the approximated radiological density in g/cm^3. ρ_{app} is the apparent density of the bone, in kg/m3.

$$\rho_{ash} = 0.87\rho_{QTC} + 0.079 \quad (9)$$
$$\rho_{app=}\frac{\rho_{ash}}{0.6} \quad (10)$$

3.2.3 Boundary conditions

A lateral fall was simulated for both fracture and control specimens. The distal extremity of the model was fixed, and the surface of the greater trochanter was constrained in the direction of the force. The fall force was mediolateral and was distributed on the medial

nodes of the femoral head [27]. The Heigh and weight of the patients were taken into consideration to have a patient-specific fall force F_{fall} (see Figure 7).

$$F_{fall} = \sqrt{2 \cdot g \cdot h_c \cdot k_{tissue} \cdot m} \qquad (11)$$
$$h_c = 0.51 \cdot h \qquad (6)$$

where g is the gravity acceleration field ($9.81\ m/s^2$), k_{tissue} is a constant related to the unidirectional stiffness of the soft tissues that cover the trochanter ($71N/mm$), m is the mass of the patient, and h_c is the height of the center of gravity related to the height of the patient h [27].

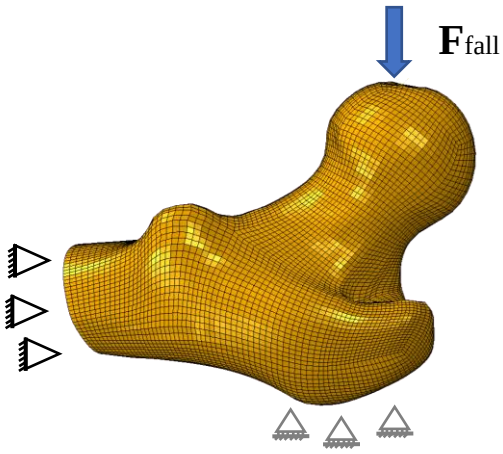

Figure 7: Bounday conditions applied to simulate a lateral fall

All the meshes and simulations were done using the Abaqus v2018 software[2].

The variables extracted for each element of each model were the following:

- Volumetric bone mineral density (vBMD)
- Major Principal Stress (MPS) [MPa]
- Major Principal Strain (MPE) [mm/mm]
- Maximum principal stress absolute [MPa]
- Maximum principal strain absolute [mm/mm]

3.3 Data preparation

The data from the new simulation was put together with the one of the previous study. This was possible since the same one-to-one node correspondence was applied in both studies.

As mentioned earlier, each model had 126800 hexahedral elements which included both cortical and trabecular bone. As to reduce the dimensionality of our data for further analysis and focus only on the relevant regions regarding the fractures, only the elements

[2] https://www.3ds.com/es/productos-y-servicios/simulia/productos/abaqus/

located in the neck and trochanteric region of the models were selected. Nevertheless, those elements that were part of the boundary conditions (BC) were not considered. Below the region under study and the number of elements of each tissue are shown.

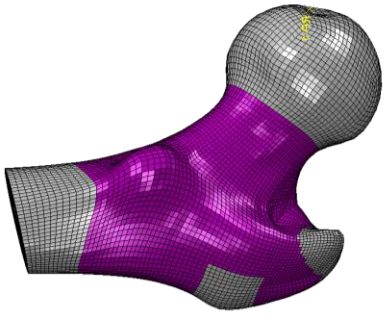

Figure 8: Neck and trochanter regions without the elements that are part of the BC

Type of bone	Number of elements
Cortical	16353
Trabecular	68372
Total elements	84680

Table 2: Elements selected for the statistical analysis

To find those regions that showed statistically significant differences between groups so that predictions could be done only by looking at those regions the threshold for the statistical tests needed to be found. For this, the 'smp1d'[3] MATLAB[4] package was used. Spm1d is a package for one-dimensional Statistical Parametric Mapping (SPM) which uses random field theory.

From the models, a three-dimensional geometry was used. As the "smp1d" package works only with 1D continuous inputs, a transformation from a 3D coordinate system to a 1D ordered sequence of elements needed to be done. This transformation was done as in [12] and was implemented with MATLAB. The path followed a logical order based on the minimum distance between the nodes of the elements and no node was considered twice in the path. To be able to analyze separately the cortical and trabecular bone, two different paths were created, one for each type of bone tissue, still the possibility of merging the two paths to create a single path for the whole geometry was also possible. In the image below the paths following the trabecular bone and cortical bone nodes are shown as well as the path combining both.

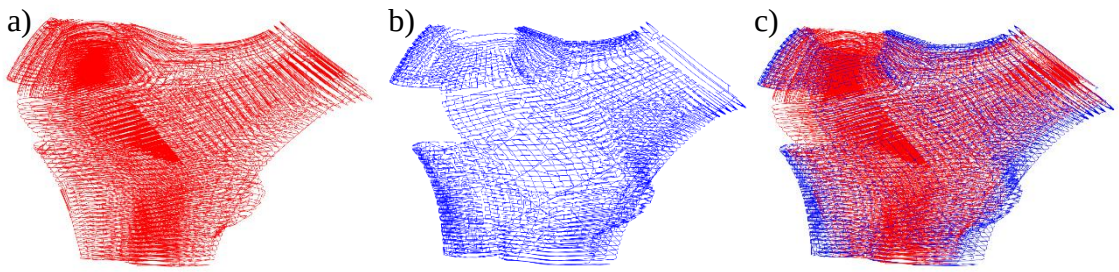

Figure 9:a) Path of the trabecular bone, b) Path of the cortical bone, c) Path of trabecular and cortical bone

[3] https://spm1d.org/

[4] https://es.mathworks.com/products/matlab.html

3.4 Statistical analysis of 1D continua: Two-way ANOVA test within Statistical Parametric Map

Through RFT, different two-way ANOVA tests were performed with 'spm1d' to examine the effects of the stress, the strain, the MPS, the MPE and the vBMD. As the RFT methodology stated, firstly a smoothness of the data was required. In this case, two different smoothness were performed to compare the outcomes between them. One used the full width of half-maximum (FWHM) of a Gaussian kernel of 10 elements and the other of 20 elements.

The 'spm1d' software implemented the RFT using an α value of 0.01 since 5 variables of interest were analyzed $(\frac{0.05}{5} = 0.01)$

In these tests, the two independent variables were considered: the gender (female vs male cases) and the condition (control group vs fractured groups). As there are two different regions where the fractures occur, the different ANOVA tests only considered on type of fracture (neck or trochanter) at the time. Also, a distinction between tissues was considered, and a different test for each tissue was done.

The different tests performed can be summarized in Table 3, these tests were performed twice, one with the dataset with the smoothness of 10 and another with the data with the smoothness of 20:

From these tests, we obtained the cluster of elements of the paths that were statistically significant for each independent variable. These clusters were a group of contiguous elements of the path that had an F value higher than the threshold found using the RFT. Also, with this test, we could also identify those elements that showed an interaction between the two independent variables (gender and femur condition).

To be able to perform a classification that could be generalized among both genders, the fewer interactions between the gender and the femur condition, the better. Having no interactions would mean that, if the gender of the patient influences the medical condition it will do it in the same constant way in the two different groups. To quantify these interactions, the percentage of the statistically significant elements of the condition test that were shared with the gender test were calculated

	Two-way ANOVA		Variable condition	Variable gender
Stress	1		Control vs. neck fracture	Female vs. male
		1.a	CORTICAL	
		1.b	TRABECULAR	
	2		Control vs. trochanter fracture	Female vs. male
		2.a	CORTICAL	
		2.b	TRABECULAR	
Strain	3		Control vs. neck fracture	Female vs. male
		3.a	CORTICAL	
		3.b	TRABECULAR	
	4		Control vs. trochanter fracture	Female vs. male
		4.a	CORTICAL	
		4.b	TRABECULAR	
MPS	5		Control vs. neck fracture	Female vs. male
		5.a	CORTICAL	
		5.b	TRABECULAR	
	6		Control vs. trochanter fracture	Female vs. male
		6.a	CORTICAL	
		6.b	TRABECULAR	
MPE	7		Control vs. neck fracture	Female vs. male
		7.a	CORTICAL	
		7.b	TRABECULAR	
	8		Control vs. trochanter fracture	Female vs. male
		8.a	CORTICAL	
		8.b	TRABECULAR	
vBMD	9		Control vs. neck fracture	Female vs. male
		9.a	CORTICAL	
		9.b	TRABECULAR	
	10		Control vs. neck fracture	Female vs. male
		10.a	CORTICAL	
		10.b	TRABECULAR	

Table 3: Summary of the different two-way ANOVA test performed

3.6 Classification through binary logistic regression

All the clusters of significant elements were extracted for each test. The mean of the values (stress, strain, MPS, MPE and vBMD) of the elements belonging to each cluster were calculated for every patient. Also, the standard deviation was calculated to see the range of variability within each cluster.

Using the IBM SPSS Statistics[5] software a forward conditional binary logistic regression was performed for each type of fracture (neck and trochanter). By method of forward conditional only a selection of the input parameters will be selected in the regression,

[5] https://www.ibm.com/es-es/products/spss-statistics

those that are more significant. Each regression was done with the same number of control cases as fractured cases and male and female patients for each regression. These regressions had as inputs the means and standard deviation for each variable, cluster, and patient. Separately, the same regression was done only considering the vBMD clusters to see the power of classification of only the radiological parameter.

If the ANOVA test showed interactions between the condition and the gender exist and the regression did give us a good enough result, the separation between gender was considered.

4. Results

4.1 Two-way ANOVA test results

For each two-way ANOVA test, graphs like the one in Figure 10 were obtained. In the X axis the enumeration of the path elements can be found and in the Y axis the F* value. The ones that go above the threshold are the elements that are statistically significant. Below we can see the two-way ANOVA test for the MPS. More statistically significant trabecular bone elements can be seen in the condition test, however, in the gender test, the cortical bone tissue is the one that has more statistically significant clusters.

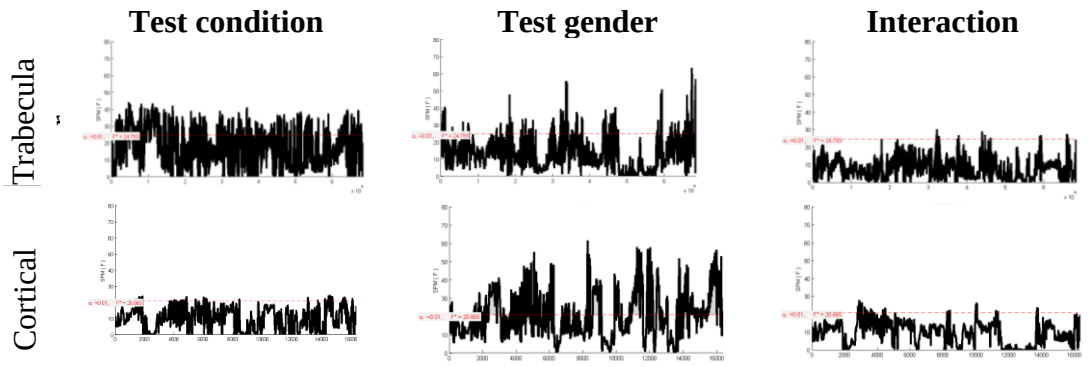

Figure 10: Two-way ANOVA test between control cases and neck fractured cases applying a Gaussian of 20 for the RFT smoothing of the MPS variable

In Table 4, the results of the number of statistically significant clusters obtained through the two-way ANOVA test can be seen. For all the variables except for the strain with a filter of 20 elements, there are more clusters in the trabecular region than in the cortical region. When comparing the results between the filter types, the smoothens done with the filter of 10 elements has more clusters, however, the clusters obtained with the Gaussian of 20 elements are formed by more elements.

The MPS variable is the one that has a higher number of statistically significant clusters of elements, and the vBMD is the variable with less clusters. There are no statistically significant regions regarding the vBMD between neck fractures and control cases, nevertheless, there are between the control cases and trochanter fracture cases.

		Number of statistical significant **clusters**			
		Control vs. neck fracture		Control vs. trochanteric fracture	
		Cortical	Trabecular	Cortical	Trabecular
Stress	Filter of 10	5	126	104	245
	Filter of 20	8	125	80	186
Strain	Filter of 10	30	14	10	15
	Filter of 20	27	17	12	10
MPS	Filter of 10	47	422	25	281
	Filter of 20	44	332	16	225
MPE	Filter of 10	3	8	15	29
	Filter of 20	4	6	12	22
vBMD	Filter of 10	0	134	12	181
	Filter of 20	0	96	9	116

Table 4: Table with the number of statistically significant cluster of elements of the different two-way ANOVA test performed.

When quantifying the interaction between gender and condition, the variables strain, MPE and vBMD did not show any interactions. The stress and MPS did show interactions as it can be seen in Table 5. Regarding the stress variable, those elements that were statistically significant in both the gender and the condition test were less than 1% of the total significant elements of the condition test. The MPS show higher percentages of elements statistically significant for both independent variables with a percentage of nearly 70%.

		Control vs. neck fracture & Female vs. male		**Control vs. trochanter fracture & Female vs. male**	
		Cortical (% of elements)	Trabecular (% of elements)	Cortical (% of elements)	Trabecular (% of elements)
Stress	Filter of 10	0	0	0	0
	Filter of 20	0	0.0 5%	0.55 %	0
MPS	Filter of 10	12.80 %	1.91 %	8.31 %	0
	Filter of 20	69.04 %	5.61 %	26.09 %	0.89 %

Table 5: Percentage of statistically significant elements form the condition test that are also statistically significant in the gender test. Stress and MPS are the only variables shown since only those present shared statistically significant elements.

When displaying the clusters of elements in the 3D geometry, it can be seen that the statistically significant regions of each fracture case (neck and trochanter) are not only in that region of fracture but in both neck and trochanter. The following figure (Figure 11)

shows the disposition of the clusters using the Gaussian of 20 elements, the figure when using the Gaussian of 10 can found in Figure S1

	Elements statistically significant in neck fractures	Elements statistically significant in trochanteric fractures
Stress	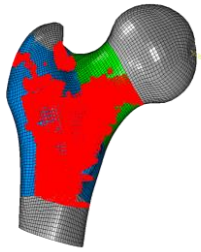	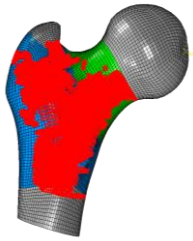
Strain	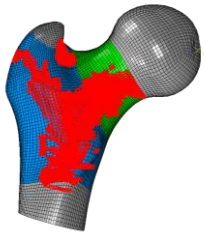	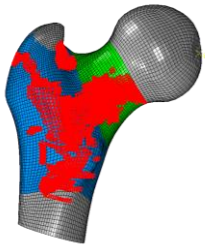
MPS	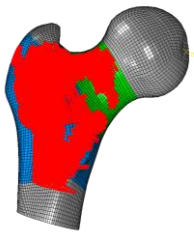	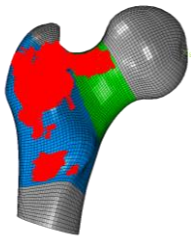
MPE	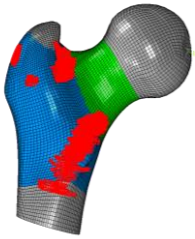	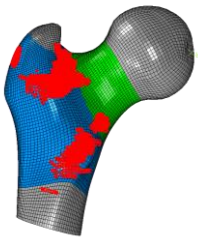
vBMD	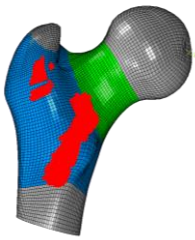	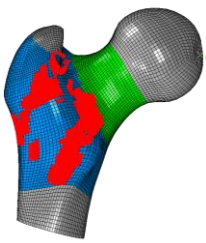

Figure 11: 3D visualization of the significant elements of cortical and trabecular bone found in the two-way ANOVA test. This are the elements obtained using the Gaussian of 20 in the smoothing of the RFT

4.2 Classification results

4.2.1 Classification by mechanical parameters

In the case of the binary logistic regression for the classification of trochanteric fractures, an accuracy of 100% was obtained with both the Gaussians filters. In Table 6, the different clusters used to achieve this classification can be seen. For the neck fractures, a 93.% accuracy was reached with both filters. The cluster that gave this classification accuracies can be found in Tab.S1. The 3D visualization of the clusters used for the prediction of trochanter and neck fracture using the 20 element Gaussian filter can be seen in Figure 12.

Gaussian of 10 elements				Gaussian of 20 elements			
Measure	**Variable**	**Bone**	**Cluster**	**Measure**	**Variable**	**Bone**	**Cluster**
Std	Stress	Trab	8	Std	Stress	Trab	68
Std	Stress	Trab	53	Std	Stress	Trab	69
Std	Stress	Trab	135	Mean	Stress	Trab	151
Std	Stress	Trab	211	Std	Stress	Cort	7
Mean	Stress	Cort	1	Std	Strain	Cort	2
Std	Strain	Trab	5	Std	MPS	Trab	68
Mean	Strain	Trab	12	Std	MPS	Trab	148
Std	Strain	Cort	1	Mean	MPS	Trab	179
Std	MPS	Trab	81	Std	MPS	Trab	185
Std	MPS	Trab	242	Mean	MPS	Cort	1
Std	MPS	Cort	18	Std	MPE	Trab	1
Std	MPE	Trab	18	Std	MPE	Trab	21
Mean	MPE	Trab	22				
Std	MPE	Trab	23				

Table 6: Clusters of the different mechanical variables obtained in the binary regression that allowed the prediction of the trochanteric fractures with an accuracy of 100% in both filters.

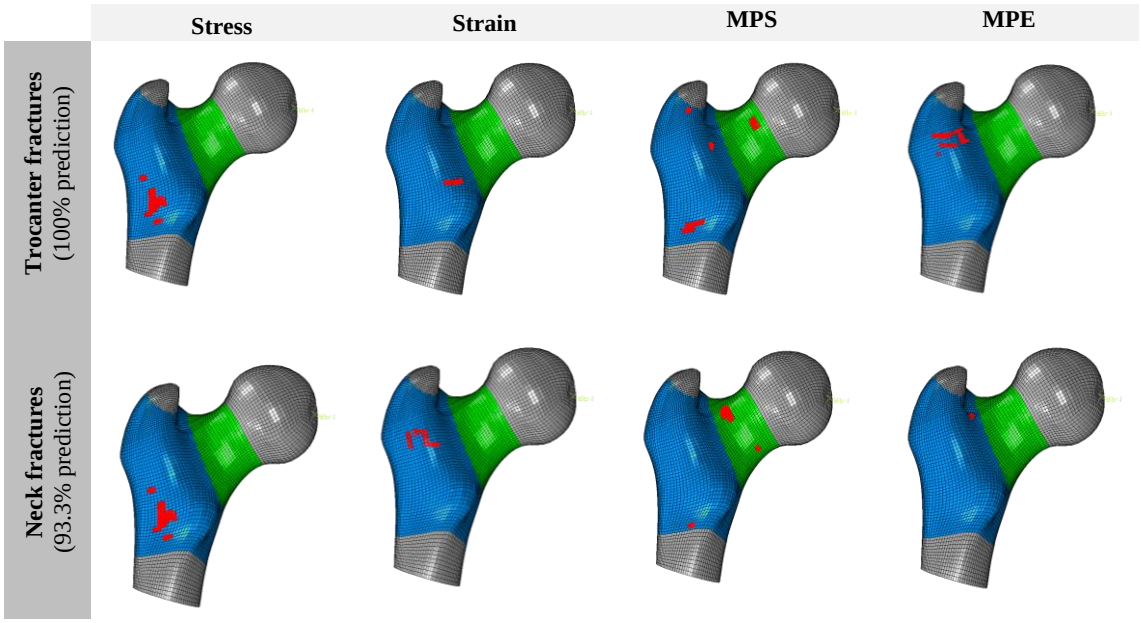

Figure 12: Clusters selected in the forward binary regression using the 20 elements Gaussian filters for the prediction of trochanteric fractures and neck fractures

To improve the neck fracture classification accuracy, a regression was done for each gender separately. With this classification, a 100% of accuracy was obtained for both

genders and filters. The cluster that used for this prediction can be seen in Figure 13 and in Table S2. Although the cluster displayed below can predict with 100% accuracy neck fractures, only the male MPS variable presents clusters in the neck region.

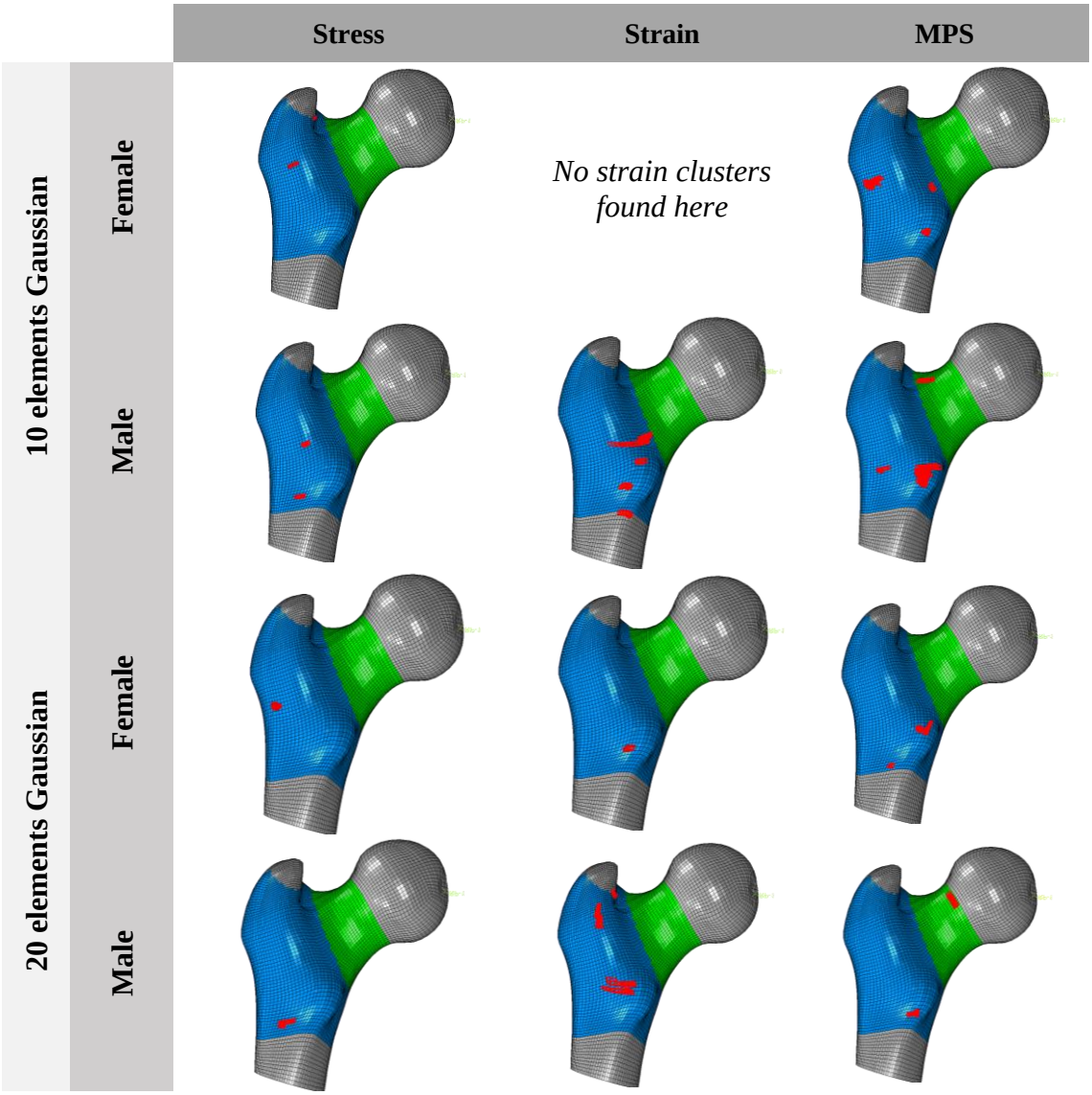

Figure 13: Cluster of elements for the variables stress, strain and MPS that where used for the binary regression classification for the prediction of neck fractures. Here the analysis is separated by genders

4.2.2 Classification by vBMD

The results of the binary logistic regression using only the vBMD as a variable gave the following results: a 74% accuracy for the prediction of neck fractures using the Gaussian filter of 10 elements smoothing and a 81,7% when using the Gaussian of 20 elements. For the trochanter fractures, a classification with an accuracy of 100% was obtained using the Gaussian smoothing of 10 elements and a 85.5% when performing it with the Gaussian of 20 elements. The clusters that allowed this percentage of accuracies for the

neck fractures and trochanteric fractures can be found in Table S3 and Table S4 respectively. In Figure 14, the different clusters obtained with the binary linear regression are highlighted in each geometry.

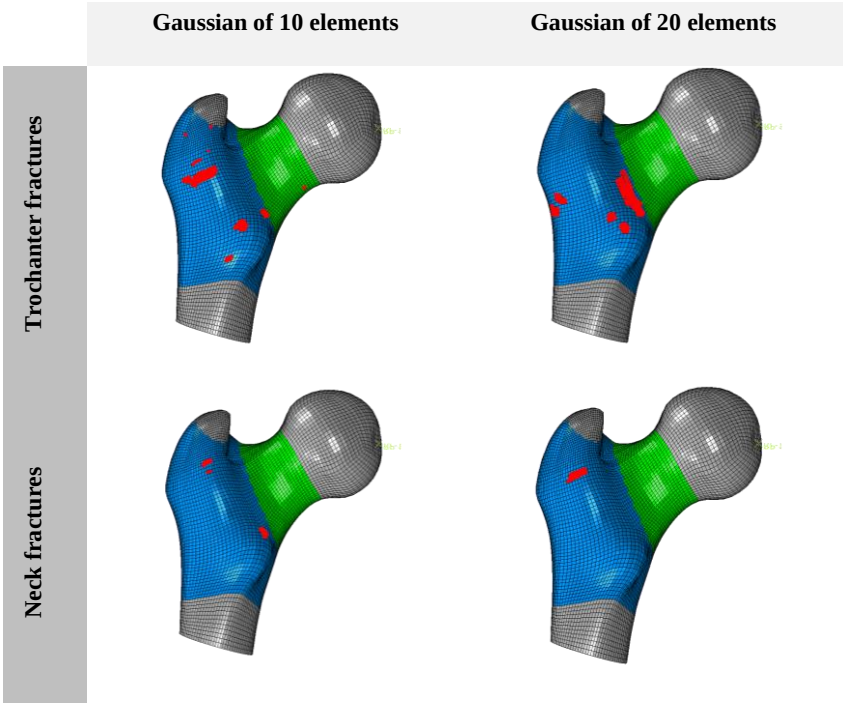

Figure 14: Clusters selected in the forward binary regression when considering only the vBMD.

After performing the different binary regressions, most of the clusters that were used for the classification belong to the trabecular bone, hence, this region is where more statistically significant differences appear between control and fractured cases. If we look at Table 6, S1, S2, S3 and S4, it can be seen that the standard deviation measure of each cluster is more frequently present than the means. With this, we can state that the distribution of values within the clusters has a great influence on the risk of suffering a fracture. When comparing the different outcomes using the two filters, the results obtained using the 10 elements Gaussians are better. This is because when more smoothing is applied, information is lost, and in this case, in the smoothing of 20 elements, information crucial for the prediction is lost.

5. Discussion

This project aimed to apply the same methodology stated in [12] in a gender and fractured balanced data set. In this study, more mechanical variable and the gender were also evaluated to see if the prediction of the risk of suffering an osteoporotic hip fracture could be improved.

When performing the different two-way ANOVA tests only the variable stress and MPS have significant elements shared between the independent variables (gender and condition) (see Table 5). As both variables quantify the tension/traction of the bone in

different manners, it makes sense that they both have interactions between gender and condition. These variables are also the ones that have the higher count of clusters among the other variables. This means that these variables are the ones that present more differences between control and fractured cases.

Trabecular bone is the tissue that showed a higher number of statistically significant clusters among all variables. This could be explained by the fact that osteoporosis is a disease that affects mainly the trabecular bone [39], and that is this trabecular bone affectation which makes it more relevant. This could be seen in the ANOVA test result regarding the vBMD, where the neck vs. control cases test shows no statistically significant clusters in the cortical bone and just a few in the trochanter vs. control cases test.

When performing the prediction using only the mechanical parameters, it can be seen that in the variable of MPS (see Figure 12), clusters can be identified in both neck and trochanteric regions for both neck and trochanter fracture predictions. In the neck fracture prediction clusters, the different clusters used for the classification are found in the trochanter region except for the MPS variable that we just mentioned that shows clusters in both regions. The cluster distribution for each classification does not intuitively suggest a reason why a fracture occurs, so a mechanical explanation on why those regions determine a fracture is represented in this project. This fact supports the theory stated in [27], where the hypothesis that the critical region could not be the ones where the fractures occur is validated.

By applying the methodology stated in [12] with a balanced dataset, not only the automatic selection of these critical regions can be achieved but also a 100% correctness of the classification can be reached. Another key step has been to evaluate the interactions between independent. This evaluation has let us perform a separate analysis by gender in the neck fractures classification which has improved our classification outcomes. With this, we can state that the gender variable affects the risk of developing an osteoporotic hip fracture.

Previous studies have focused on finding a single parameter and region that is able to predict the osteoporotic hip fracture. For example, in [12,27] they stated that MPS was the best mechanical classifier obtaining a 91% and 81% accuracies when classifying trochanter and neck fractures respectively [27]. In [34] only the strain variable was considered find the structural parameters related to the fracture. However, this study had a different approach. Instead of aiming to find single parameter, we have focused on establishing where the critical region are for different variables. This way with a combination of the difference critical regions for the different parameters, higher accuracies had been achieved.

A perfect classification is reached when considering the biomechanical parameters stress, strain, MPS, and MPE obtained from lateral fall FEM simulations. Simulations computational cost keeps away such model from regular clinical practice. However, new meshes developed in the research group have reduced the computational time. The test of the methods used in this project with the new meshes should be further explored.

An advantage of using only the vBMD is that no lateral fall simulation is needed, only the model with BMD for each element. Even though the results from the predictions using

the only vBMD are not as good as the ones using the mechanical parameters, when using the smoothing of the 10 elements Gaussians, the prediction of neck fractures and trochanteric fractures are 81,7% and 100% respectively. This percentages overcome the ones of the technique that can be easily implemented in the clinic. Those are the ones base on only clinical data [31] which was 72.17% and the current fast-predictive tool that is the FRAX (70%) [9].

Previous studies on the prediction of hip fracture have been developed using QCT images [40,41]. QCT is an imaging technique that directly measures the volumetric distribution of the BMD at cost of higher radiation. By developing FE analysis based on QCT, a 87.5% and 80% accuracy have been reached for predicting neck and trochanter fractures respectively [41]. In our study DXA scans were used. DXA scans are the tool used for the follow-up of the osteoporotic patients and are far less ionizing than QCT. Although DXA scans do not offer a 3D distribution of the BMD, the vBMD can be obtained thanks to the 3D-shaper software. When comparing the outcomes between studies, our results based on DXA scans showed higher accuracies values than those based on QCT. Apart from presenting higher predictive values, the fact that is being based on a less ionizing imaging technique, that is routinely performed on this type of patients, makes this predictive tool outstand among the others.

The fact that vBMD, obtained from the processing of DXA scans, can achieve this level of precision when predicting an osteoporotic hip fracture opens the doors to a more patient-specific treatment. With this tool, those patients that show a risk of suffering either a neck or a trochanteric fracture could start a preventive treatment to be able to reduce this risk. This will lead to smarter use of the resources since only those patients at risk would have a preventive treatment indication and with the right prevention, the number of fractures would decrease. Needless to mention the benefit for the patient, since the consequences of suffering this kind of fracture are limiting for the patient and can even lead to death.

Although this study has shown promising results, it has some limitations. The first limitation is related to the way the 1D trajectory path is created when there is more than one node with the same minimal distance, this limitation is more extensively explained in [12]. Despite, when this scenario occurs, the creation of this 1D path offer the possibility to perform analysis that with the 3D geometry could not have been achieved. This study has been done with 180 patients. The size of the data set is comparable to all the other studies performed in this topic and even superior. Nonetheless, to verify if this result can be generalized more patients should be studied. The last limitation is that to perform the binary linear regressions, the means of each cluster were calculated. As stress and strain variables can have positive or negative values, it may happen that in some clusters positive and negative values are present, and by averaging, this information is lost. Then this affects the interpretation of the results since we will know which elements can be selected to perform the classification but we are not able to explain biologically and mechanically what is happening in those regions. Therefore, in future studies, we plan to differentiate between the clusters that are at traction or tension and with a positive or negative strain. This way, the result could be more interpretable biomechanically since we will be able to identify what is happening in each cluster.

6. Conclusion

This study has proven the importance of the selection of the region under analysis. Through RFT, an automatic selection of the critical region can be done. This selection, let to a perfect prediction base on mechanical parameters. By using only, the vBMD a good classification can be obtained too. Given that vBMD can be obtained from model based on the 3D projection of the 2D DXA follow-up scans of osteoporotic patients, no patient-specific lateral fall simulation is needed. This makes this last variable the perfect candidate to be applied in clinics.

By predicting the risk of suffering an osteoporotic hip fracture, preventive treatments can be provided to patients to reduce this risk. This could be catalyst to a reduction of the social and economic burden that this medical condition causes.

BIBLIOGRAPHY

1. Chami, G., Jeys, L., Freudmann, M., Connor, L., & Siddiqi, M. (2006). Are osteoporotic fractures being adequately investigated?: A questionnaire of GP & orthopaedic surgeons. *BMC Family Practice*, *7*(1). https://doi.org/10.1186/1471-2296-7-7

2. Braithwaite, R. S., Col, N. F., & Wong, J. B. (2003). Estimating Hip Fracture Morbidity, Mortality and Costs. *Journal of the American Geriatrics Society*, *51*(3), 364–370. https://doi.org/10.1046/j.1532-5415.2003.51110.x
3. Metcalfe, D. (2020). The pathophysiology of osteoporotic hip fracture. *McGill Journal of Medicine*, *11*(1). https://doi.org/10.26443/mjm.v11i1.410
4. Johnell, O., & Kanis, J. (2004). Epidemiology of osteoporotic fractures. *Osteoporosis International*, *16*(S02), S3–S7. https://doi.org/10.1007/s00198-004-1702-6

5. Coste y resultado de la fractura de cadera osteoporótica en España. (2012, July). Mutua de Terrassa https://mutuaterrassa.com/blogs/es/traumatologia/coste-resultado-fractura-cadera-osteoporotica-espanya

6. Seeman, E. (1997, August 18). *Osteoporosis: Trials and tribulations*. The American Journal of Medicine. Retrieved January 7, 2022, from https://doi.org/10.1016/S0002-9343(97)90029-2

7. V. (2020, April 16). *Other diagnostic tools*. International Osteoporosis Foundation. https://www.osteoporosis.foundation/health-professionals/diagnosis/other-diagnostic-tools

8. Bai, D. (2020, July 30). *Calcaneal Quantitative Ultrasound May Serve as a Prescreening Tool for Osteoporosis*. AJMC. https://www.ajmc.com/view/calcaneal-quantitative-ultrasound-may-serve-as-a-prescreening-tool-for-osteoporosis

9. O. (2017, January 23). *FRAX: A Valuable Tool, But It Has Limitations*. Consult QD. https://consultqd.clevelandclinic.org/frax-a-valuable-tool-but-it-has-limitations/

10. J. Fish, T. Belytschko. A First Course in Finite Elements. Wiley. 2007. ISBN: 978-0470035801

11. Ruiz Wills, C., Tassani, S., di Gregorio, S., Martínez, S., González Ballester, M., Humbert, L., Noailly, J., & Río, L. D. (2020). Fragilidad relativa de fémures osteoporóticos evaluados con DXA y simulación de caídas con elementos finitos guiados por radiografías de urgencias. *Revista de Osteoporosis y Metabolismo Mineral*, *12*(2), 62–70. https://doi.org/10.4321/s1889-836x2020000200005

12. N. Morando (2021). Identification of statistical critical area of proximal femur when a lateral fall happens. *Master Thesis*

13. Cht, O. T. S. M., Md, L. O. A., Atc, F. J. P. P. C., Md, P. A. C., Felder, S., & Shin, E. K. (2020). *Rehabilitation of the Hand and Upper Extremity, 2-Volume Set: Expert Consult: Online and Print* (7th ed.). Elsevier.

14. Cody, D. D., Hou, F. J., Divine, G. W., & Fyhrie, D. P. (2000). Femoral structure and stiffness in patients with femoral neck fracture. *Journal of Orthopaedic Research*, *18*(3), 443–448. https://doi.org/10.1002/jor.1100180317

15. *Bone Biopsies: A Modern Approach*. (1998, January 1). ScienceDirect. https://www.sciencedirect.com/science/article/pii/B9780120687008500098

16. Caeiro, J., González, P., & Guede, D. (2013). Biomecánica y hueso (y II): ensayos en los distintos niveles jerárquicos del hueso y técnicas alternativas para la determinación de la resistencia ósea. *Revista de Osteoporosis y Metabolismo Mineral*, *5*(2), 99–108. https://doi.org/10.4321/s1889-836x2013000200007

17. Lumen Learning & OpenStax. (n.d.). *Bone Structure | Anatomy and Physiology I*. Lumen. https://courses.lumenlearning.com/hccs-ap1/chapter/bone-structure/

18. *The Femur - Proximal - Distal - Shaft*. (2020, November 13). TeachMeAnatomy. https://teachmeanatomy.info/lower-limb/bones/femur/

19. *What is the anatomy relative to intertrochanteric hip fractures?* (2021, October 16). Medscape. https://www.medscape.com/answers/1247210-87285/what-is-the-anatomy-relative-to-intertrochanteric-hip-fractures

20. R. (2018, September 12). *Osteoporosis. Definición. Epidemiología*. Revista de Osteoporosis y Metabolismo Mineral · Publicación Oficial SEIOMM. http://revistadeosteoporosisymetabolismomineral.com/2017/07/11/osteoporosis-definicion-epidemiologia/

21. Manolagas, S. C. (2013, December 28). *Cellular and molecular mechanisms of osteoporosis*. SpringerLink. https://doi.org/10.1007/BF03339652

22. Geng, C. (2021, November 30). *What is secondary osteoporosis?*. https://www.medicalnewstoday.com/articles/secondary-osteoporosis#primary-vs-secondary

23. Melmed, S., Koenig, R., Rosen, C. J., Auchus, R., & Goldfine, A. B. (2019). *Williams Textbook of Endocrinology*. Elsevier Gezondheidszorg.

24. *Bone Mass Measurement: What the Numbers Mean | NIH Osteoporosis and Related Bone Diseases National Resource Center*. (2018, October 1). NIH Osteoporosis and Related Bone Diseases Nationa Resources Center. https://www.bones.nih.gov/health-info/bone/bone-health/bone-mass-measure

25. Choksi, P., Jepsen, K. J., & Clines, G. A. (2018). The challenges of diagnosing osteoporosis and the limitations of currently available tools. *Clinical Diabetes and Endocrinology*, *4*(1). https://doi.org/10.1186/s40842-018-0062-7

26. Ramos, R. L. M. (2012, September 1). *Absorciometría con rayos X de doble energía. Fundamentos, metodología y aplicaciones clínicas | Radiología*. ELSEVIER. https://www.elsevier.es/es-revista-radiologia-119-articulo-absorciometria-con-rayos-x-doble-S0033833811003729

27. Ruiz Wills, C., Olivares, A. L., Tassani, S., Ceresa, M., Zimmer, V., González Ballester, M. A., del Río, L. M., Humbert, L., & Noailly, J. (2019). 3D patient-specific finite element models of the proximal femur based on DXA towards the classification of fracture and non-fracture cases. *Bone*, *121*, 89–99. https://doi.org/10.1016/j.bone.2019.01.001

28. Acr, R. A. (2021, July 30). *Bone Densitometry (DEXA, DXA)*. Radiologyinfo.Org. https://www.radiologyinfo.org/en/info/dexa

29. Harding, M. (2018, March 12). *DXA Scan*. https://patient.info/bones-joints-muscles/osteoporosis-leaflet/dexa-scan

30. Education, O. M. (2016, April 18). *Hip Fractures: Intracapsular Neck of Femur Fractures*. Oxford Medical Education. https://oxfordmedicaleducation.com/surgery/trauma-and-orthopaedics/intracapsular-neck-of-femur-fractures/

31. Villamor, E., Monserrat, C., del Río, L., Romero-Martín, J., & Rupérez, M. (2020). Prediction of osteoporotic hip fracture in postmenopausal women through patient-specific FE analyses and machine learning. Computer Methods and Programs in Biomedicine, 193, 105484. https://doi.org/10.1016/j.cmpb.2020.105484

32. *Introduction to finite element analysis*. (n.d.). OpenLearn. https://www.open.edu/openlearn/science-maths-technology/introduction-finite-element-analysis/content-section-1.5

33. Fleps, I., Enns-Bray, W. S., Guy, P., Ferguson, S. J., Cripton, P. A., & Helgason, B. (2018). Correction: On the internal reaction forces, energy absorption, and fracture in the hip during simulated sideways fall impact. *PLOS ONE*, *13*(11), e0208286. https://doi.org/10.1371/journal.pone.0208286

34. Aldieri, A., Terzini, M., Osella, G., Priola, A. M., Angeli, A., Veltri, A., Audenino, A. L., & Bignardi, C. (2018). Osteoporotic Hip Fracture Prediction: Is T-Score-Based Criterion Enough? A Hip Structural Analysis-Based Model. Journal of Biomechanical Engineering, 140(11). https://doi.org/10.1115/1.4040586

35. Flandin, G., & Friston, K. (2008). Statistical parametric mapping (SPM). Scholarpedia, 3(4), 6232. https://doi.org/10.4249/scholarpedia.6232

36. Penny, W. D., Friston, K. J., Ashburner, J. T., Kiebel, S. J., & Nichols, T. E. (2006). Statistical Parametric Mapping: The Analysis of Functional Brain Images (1st ed.). Academic Press.

37. Brett, M., Penny, W., & Kiebel, S. (2003). Introduction to random field theory. Human brain function, 2, 867-879.

38. Lani, J. (2021, August 3). Bonferroni Correction. Statistics Solutions. https://www.statisticssolutions.com/bonferroni-correction/

39. Osterhoff, G., Morgan, E. F., Shefelbine, S. J., Karim, L., McNamara, L. M., & Augat, P. (2016). Bone mechanical properties and changes with osteoporosis. Injury, 47, S11–S20. https://doi.org/10.1016/s0020-1383(16)47003-8

40. Adams, A. L., Fischer, H., Kopperdahl, D. L., Lee, D. C., Black, D. M., Bouxsein, M. L., Fatemi, S., Khosla, S., Orwoll, E. S., Siris, E. S., & Keaveny, T. M. (2018). Osteoporosis and Hip Fracture Risk From Routine Computed Tomography Scans: The Fracture, Osteoporosis, and CT Utilization Study (FOCUS). Journal of Bone and Mineral Research, 33(7), 1291–1301. https://doi.org/10.1002/jbmr.3423

41. Nishiyama, K. K., Ito, M., Harada, A., & Boyd, S. K. (2013). Classification of women with and without hip fracture based on quantitative computed tomography and finite element analysis. *Osteoporosis International*, *25*(2), 619–626. https://doi.org/10.1007/s00198-013-2459-6

SUPPORTING INFORMATION

Classification clusters

Gaussian of 10 elements				Gaussian of 20 elements			
Measure	**Variable**	**Bone**	**Cluster**	**Measure**	**Variable**	**Bone**	**Cluster**
Mean	Strain	Trab	5	Std	Stress	Trab	13
Mean	Strain	Trab	7	Std	Stress	Trab	32
Std	Strain	Cort	4	Mean	Stress	Trab	91
Std	MPS	Trab	18	Mean	Stress	Trab	107
Mean	MPS	Trab	98	Std	Strain	Cort	6
Std	MPS	Trab	192	Std	MPS	Trab	97
Std	MPS	Trab	238	Std	MPS	Trab	199
Std	MPS	Cort	30	Mean	MPS	Trab	301
Mean	MPE	Trab	7	Std	MPE	Cort	1

Table S1: Clusters of the different mechanical variables obtained in the binary regression that allowed the prediction of the neck fractures with an accuracy of 93.3% in both filters

	Female variables				Male variables			
	Measure	**Variable**	**Bone**	**Cluster**	**Measure**	**Variable**	**Bone**	**Cluster**
Gaussian 10	Std	Stress	Trab	26	Mean	Stress	Trab	69
	Std	Stress	Cort	2	Mean	Stress	Trab	95
	Mean	MPS	Trab	14	Std	Strain	Trab	9
	Std	MPS	Trab	28	Std	Strain	Cort	3
	Mean	MPS	Trab	311	Mean	Strain	Cort	4
	Mean	MPS	Trab	406	Std	Strain	Cort	11
					Std	MPS	Trab	21
					Std	MPS	Trab	299
					Std	MPS	Cort	17
Gaussian 20	Mean	Stress	Trab	114	Mean	Stress	Trab	95
	Std	Strain	Trab	11	Std	Stress	Trab	107
	Std	MPS	Cort	119	Mean	Strain	Trab	17
	Mean	MPS	Trab	301	Std	Strain	Cort	10
					Std	Strain	Cort	24
					Std	MPS	Trab	3
					Std	MPS	Trab	168
					Std	MPS	Trab	235

Table S2: Cluster that were selected in de forward binary regression for the neck fracture when performing the prediction with gender separation. This table show the cluster for each gender and each filter used

Gaussian of 10 elements			Gaussian of 20 elements		
Measure	**Bone**	**Cluster**	**Measure**	**Bone**	**Cluster**

Std	Trab	36	Std	Trab	23
Std	Trab	37	Mean	Trab	32
Std	Trab	58	Mean	Trab	41
Mean	Trab	78			
Mean	Trab	134			

Table S3: Cluster obtained in the binary linear regression for the prediction of neck fractures using only the vBMD as input variable

Gaussian of 10 elements			Gaussian of 20 elements		
Measure	**Bone**	**Cluster**	**Measure**	**Bone**	**Cluster**
Std	Trab	18	Std	Trab	14
Std	Trab	21	Std	Trab	47
Mean	Trab	50	Std	Trab	61
Std	Trab	73	Std	Trab	64
Std	Trab	94	Std	Trab	114
Std	Trab	103	Std	Cort	3
Std	Trab	115			
Std	Trab	119			
Std	Trab	146			
Mean	Trab	180			

Table S4: Cluster obtained in the binary linear regression for the prediction of trochanteric fractures using only the vBMD as input variable

Clusters visualization

	Elements statistically significant in neck fractures	Elements statistically significant in trochanteric fractures
Stress	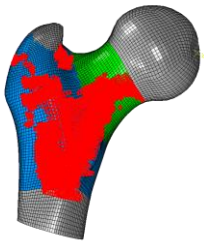	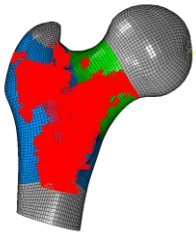
Strain	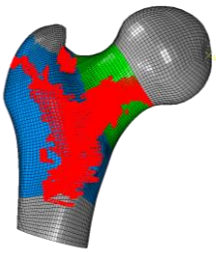	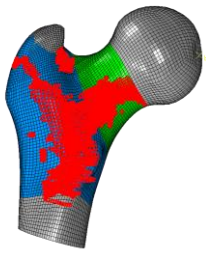
MPS	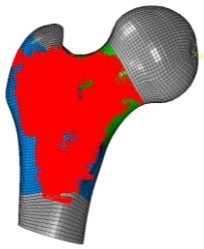	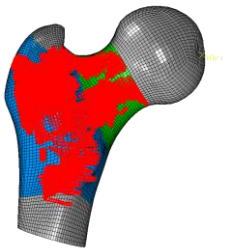
MPE	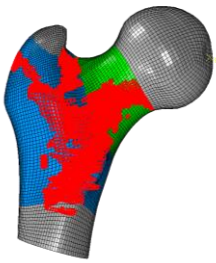	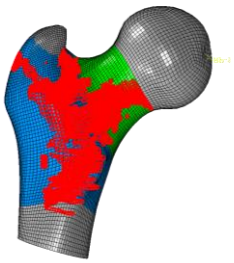
BMD	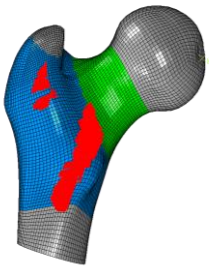	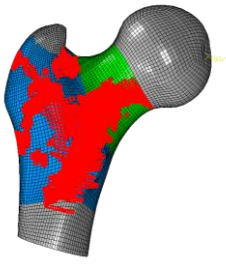

Figure S1: 3D visualization of the significant elements of cortical and trabecular bone found in the two-way ANOVA test. This are the elements obtained using the Gaussian of 10 in the smoothing of the RFT